Check for updates

Recyclable construction of multi-layer films with an impedance gradient design for high-efficiency electromagnetic absorption performance†

Yu Chen,[a] Bin Quan, ![ID] *[a] Litao Lin,[a] Linyu Xie,[d] Haoyu Jiao,[a] Xinyi Min,[c] Gaoyuan Yu,[a] Binglin He,[e] Xiaochi Lu,[b] Jiajia Liu,[a] Yan Chen[a] and Xiaogu Huang*[a]

This work presents the first recyclable multi layer films with an impedance optimization design, created *via* simulation screening, that consists of films ordered and arranged to enhance the absorption bandwidth from 0 GHz to 2.17 GHz. The results presented here provide valuable insights into the design and construction of high-efficiency microwave absorption films by environmentally friendly and sustainable technological means.

With the proliferation of electronic devices and the rapid development of wireless communication technologies, issues surrounding electromagnetic (EM) wave radiation has become increasingly prominent.[1] EM wave absorption materials can effectively absorb and reduce the reflection and scattering of EM waves, thereby mitigating EM interference, safeguarding the normal operation of electronic devices, and concurrently reducing the harm on human health.[2] However, it is difficult to effectively recover and repair the most widely applied EM wave absorption materials. Meanwhile, structural design is required to achieve more efficient EM wave absorption performance.[3]

EM wave absorption films are finding ever-wider applications in electronic devices due to their lightweight characteristics. Thin film materials can be conveniently coated or adhered to the surfaces of various electronic devices, providing effective EM shielding and absorption. The main way to construct the structures is by multi-layer coating.[4] The difference in the component ratio and EM performance between each layer provides a

possible way to reach higher performance.[5] For instance, the design of a multi-layer film structure takes advantage of the reflection, refraction, and absorption characteristics of different material layers, and through optimized design, efficient absorption of EM waves within specific frequency ranges can be realized.[6] Such a design not only enhances the absorption performance but also enables selective control of the absorption frequency. With the growing awareness of environmental protection and the increasing scarcity of resources, recyclable multi-layer film designs have assumed greater significance.[7] By adopting recyclable or degradable materials and designing structures that are facile to separate and reuse, the impact of electronic waste on the environment can be reduced, and the sustainable utilization of resources can be achieved.[8]

Thermoplastic elastomers (TPE) are highly recyclable plastics that can not only be physically cut into pieces for recycling but also be dissolved and separated using chemical methods.[9] Heng *et al.* realized the recovery of a carbon fiber fabric (CFF) and TPE in DMF *via* an ultrasonic-assisted solvent method, and both the CFF and TPE retained about 90% of their original properties after recovery.[10] For EM wave-absorbing materials, the presence of dielectric components and magnetic components often increases the difficulty of the recovery process.[11] The ability of TPE to dissolve completely in cyclohexane allows the substrate to be mixed or separated from the dielectric and magnetic components, which allows the incorporation of various EM absorbers with different properties in conjunction with efficient recycling. The tight bonds between the layers of multilayer films can also be easily solved by micro-dissolution and solidification of the film surface. In this process, the TPE itself acts as both a substrate and an adhesive, avoiding the introduction of additional variables affecting the EM wave absorption performance.

An effective way to achieve high performance EM wave absorption and high recovery performance is to prepare an EM wave absorption film using TPE as the substrate. The structural design can be customized to the required frequency band as a means of EM wave regulation.[12] A multilayer structure design based on an impedance matching (IM) strategy helps EM

[a] *School of Chemistry and Materials Science, Nanjing University of Information Science & Technology, Nanjing, 210044, China. E-mail: binquan@nuist.edu.cn, hxg@nuist.edu.cn*

[b] *College of Electronic and Optical Engineering & College of Flexible Electronics (future Technology), Nanjing University of Posts and Telecommunications, Nanjing, 210023, China*

[c] *JiangSu JACK Instrument Co., Ltd, 211600, China*

[d] *School of Communications and Information Engineering, Nanjing University of Posts and Telecommunications, 210023, China*

[e] *School of Computer engineering, Tongda College of Nanjing University of Posts and Telecommunications, 225127, China*

† Electronic supplementary information (ESI) available. See DOI: https://doi.org/10.1039/d4cc06768a

waves to enter the interior of the material and provides opportunities for the absorption by the strong absorbing layer.[13] To solve the need for high performance and convenient recovery, a multi-layer film structure based on TPE is proposed. CNTs have high chemical stability and can remain stable in a variety of chemical environments. They have a certain tolerance to acids and bases, which means that carbon nanotubes in polymer composites not only improve the dielectric properties of the material but also improve the acid resistance and oxidation resistance of the material. In this work, multi-layer films are innovatively combined tightly with each other, and optimal absorption performance is realized through the use of simulation and predictions. The relationship between the absorption properties of the layered structure and the basic method used to create the layered structure are studied and explained. The performance difference with and without the designed structure is tested and verified, demonstrated by the bandwidth expansion from x–y GHz to 8.2–12.4 GHz. This work successfully prepares multilayer films by enhancing the interlayer bonding *via* physical interactions, which lays a foundation for the construction of more complex multilayer films with high-efficiency EM wave absorption performance. Furthermore, the design of recyclable multi-layer films is of considerable value for environmental protection and resource conservation.

The XRD patterns of the films were obtained to confirm the successful preparation of multiple films. As shown in Fig. 1a and b, the characteristic peaks of the CNTs are at $25.8°$ and $42.7°$, corresponding to the 002 and 100 crystal planes. The peaks at $30.3°$, $35.7°$, $43.4°$, $53.8°$, $57.4°$, $63.0°$, and $74.8°$ belong to γ-Fe$_2$O$_3$.[14] The TPE peak is concentrated around $18°$, which exists in the form of a broad peak. The peak position of each material can be found in the XRD patterns. Because TCF1 has the highest relative content of TPE, the broad peak at $18°$ shows a higher relative intensity. The peak intensity of γ-Fe$_2$O$_3$ at $35.7°$ varies in line with the content of γ-Fe$_2$O$_3$ in each film. To characterize the thermal stability of the films, the TCF films were heated in nitrogen to obtain the thermogravimetric analysis curves (Fig. 1c). When the temperature is below 100 °C, the TCF films have good stability and do not decompose, indicating they can maintain sufficient stability for use in practical applications. As the temperature rises, the TPE gradually breaks down into water and

carbon dioxide. The equation of this reaction is $2(C_8H_8 \cdot C_4H_6)_n + 31O_2 \rightarrow 24nCO_2\uparrow + 14nH_2O$. To analyze the magnetic properties of the TCF films, the hysteresis loops were obtained using VSM tests (Fig. 1d and f). The magnetic component is mainly the magnetic part of the electromagnetic parameters, and because α-Fe$_2$O$_3$ does not have magnetism, in this work, the magnetic material γ-Fe$_2$O$_3$ was used. The reason for the significant difference between the two is mainly the conversion of diamagnetism to ferromagnetism caused by the phase transition. There is not a significant difference in the coercivity, mainly because the γ-Fe$_2$O$_3$ providing the magnetism does not display a significant difference, while the saturation magnetization and residual magnetization are greatly affected. The mass ratio of γ-Fe$_2$O$_3$ in films TCF1-4 are 8.77%, 27.78%, 7.94%, and 25.64%, respectively, and the VSM characterization results are consistent with these proportions and the XRD results. Additionally, SEM was used to characterize the elemental distribution and uniformity on the surface of the films (Fig. S2, ESI†). Obviously, there is less C and Fe in TCF1 and TCF3 than in TCF2 and TCF4. In contrast, the C content in TCF1 and TCF3 is higher than that of the other two films. Compared with the C element in TCF4 and TCF1, the C element is increased due to the presence of additional CNTs. As shown by various characterization methods, the components of the TCF films are consistent with their design.

The EM properties of each single TCF film were tested using the waveguide method. To achieve better EM wave absorbing performance, dielectric and magnetic losses play critical roles. Regulating the EM properties is an effective approach to adjusting those losses. CNTs provide a conductive path and γ-Fe$_2$O$_3$ a magnetic core, and are thus usually applied in EM field absorption materials.[15,16] However, the preparation of sufficiently uniform films, in this case, those of constant thickness, is often not the optimal choice. Using structural design can often achieve unexpected performance improvements. Based on the differences in the TCF films, an effective method to construct a four-layer film structure is by rearrangement. The EM properties are shown in Fig. S3a–d (ESI†), and due to the increase in CNTs content, the complex dielectric constant changes over a large range. The real part can reach 22.0 from 4.0 and the imaginary part can reach 12.0 from about 0.0. As the permeability of γ-Fe$_2$O$_3$ is relatively low, the complex permeability does not exhibit an obvious difference. The reflection loss (RL) and impedance matching value of each TCF film were calculated (Fig. S3e–l, ESI†), and when the CNTs content is consistent the RL and IM were similar. At the lowest IM value (TCF1 at 9.0 GHz and TCF2 at 9.6 GHz), significant absorption peaks were observed. When the CNTs content is high, the IM value was substantially optimized within the 8.2–12.4 GHz range, and the interaction between the material and the EM waves is enhanced. TCF1 exhibits similar IM curves at different thicknesses, with IM values closest to zero at 9.09 GHz that gradually changed with thickness to reach an optimal value at 3.5 mm (Fig. S3e, ESI†). TCF2 exhibits similar curves to TCF1, achieving the optimal IM value at 9.71 GHz at 3.0 mm (Fig. S3f, ESI†). TCF3 demonstrated much lower IM values due to the addition of the CNTs (Fig. S3g, ESI†). When adding γ-Fe$_2$O$_3$, the IM value of TCF4 increased to about 2.0 (Fig. S3h, ESI†). Among the
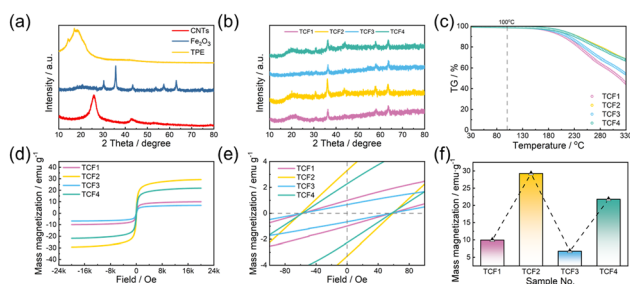

Fig. 1 Characterization of the thin films. (a) Individual XRD patterns of each component in the TCF film; (b) XRD characterization of thin films TCF1-4; (c) thermogravimetric analysis of films TCF1-4 in air; (d) saturation magnetization of films TCF1-4; (e) coercivity and remanent magnetization of films TCF1-4; and (f) saturation magnetization of films TCF1-4.

TCF films, TCF3 and TCF4 possess better RL performance than TCF1 and TCF2, although the performance between the two is also different (Fig. S3i–l, ESI†). From the Cole–Cole semicircles, it is evident that the TCF films with different ratios exhibit distinct loss mechanisms, with significant differences observed between the four TCF films (Fig. S4, ESI†). The C_0 values and attenuation constants (α) were calculated (Fig. S5 and S6, ESI†), showing that TCF4 demonstrated stronger eddy current loss characteristics compared to TCF1-3, primarily due to the large amount of γ-Fe_2O_3 it contains. However, TCF3 exhibits a higher α value, as the addition of a large amount of γ-Fe_2O_3 also led to an attenuation of the dielectric properties of TCF4. These data show that TCF1 and TCF2 have high IM values, TCF3 exhibits a strong loss to EM waves, and the loss ability of TCF4 is lower than that of TCF3.

The construction of multilayer EM wave absorbing films requires a strong connection between the layers. TPE based on TCF films can meet this requirement, and TPE can be dissolved in cyclohexane. Using this property, the TCF films can be recycled and reshaped (Fig. S7, ESI†). The recyclable construction is mainly based on remolding, using cyclohexane to dissolve the discarded TCF film. The addition of further TPE, CNTs and γ-Fe_2O_3 to the dispersion solution can be used to adjust the dielectric properties and magnetic properties. A small amount of cyclohexane was coated to the film, and thus the film will be slightly dissolved. When the cyclohexane evaporates, the TPE will transform from a liquid to a solid, and the layers close to each other will be bonded (Fig. 2). The conversion process is very rapid, and heating contributes to further volatilization of the cyclohexane. Taking TCF1 and TCF2 as examples, as shown in Fig. S8a (ESI†), a tightly joined band can be formed after connecting these two films. The film is strong enough that when it is passed through the hole of a hydrothermal autoclave reactor, it can lift it up and its original integrity is preserved (Fig. S8b, ESI†). As shown in Fig. S9 (ESI†), the cross section between the two layers bonded by cyclohexane is clear, with no significant faults. When the TCF1 and TCF2 connection is stretched (Fig. S8c, ESI†), the deformation of the two sections is different due to the difference in composition, but it still remains tightly bonded. To take advantage of this characteristic, a pre-prepared single layer TCF film can be stacked in a certain order, and the interfaces can be treated with cyclohexane to obtain a film with a four-layered structural design. The cyclohexane does not change before and after making the film, and the recycling of cyclohexane gas can not only effectively reduce the cost of the molding process but also helps to protect the environment.

The model involved in the simulation is shown in Fig. 3a, which consists of four layers of a thin film structure and two vacuum layers. Each combination is labelled with a four-digit number, where the digits represent the identification numbers of the TCF films. For example, TCF1324 means that the four-
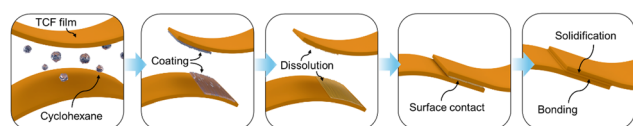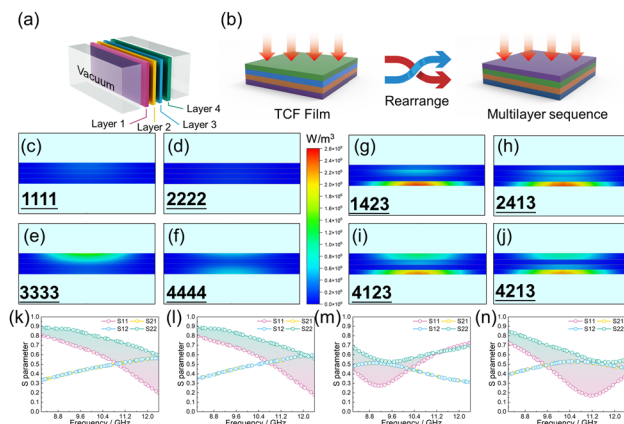

Fig. 3 (a) The simulation model; (b) multi-layer replacement strategy; the PLD value distribution diagrams of (c) TCF1111, (d) TCF2222, (e) TCF3333, (f) TCF4444, (g) TCF1423, (h) TCF2413, (i) TCF4123, and (j) TCF4213; and (k)–(n) S parameters of TCF1423, TCF2413, TCF4123, and TCF4213.

layer structure is composed of TCF1, TCF3, TCF2, and TCF4 from top to bottom, respectively. As shown in Fig. 3b, different structures can be built by swapping any two layers of the films. As shown in Fig. S10 and S11 (ESI†), simulations of the electric and magnetic field distributions were conducted for the TCF films. When the phase changes, the intensity of the magnetic fields is greatly diminished. Due to the different ratio of γ-Fe_2O_3 in the films, the magnetic field is confined to a certain depth. The magnetic field distribution of the four types of TCF films is greatly influenced by the properties of the films themselves. TCF3 achieves the maximum dissipation of the magnetic-field component of the EM wave when the EM wave penetrates to the same depth, while the electric-field component stays the same at the same depth of penetration. The S parameters were also simulated and are shown in Fig. S12 (ESI†), where absorption values between $1-S11^2-S21^2$ were obtained. Among the multi-layers films, TCF4123 and TCF4213 show the strongest EM wave absorption capability. The frequency of the strongest absorption peaks is near 10.6 GHz, and thus the power loss density (PLD) was simulated at 10.6 GHz. Firstly, simulations were conducted based on the homogeneous TCF films, TCF1111, TCF222, TCF333, and TCF444. As shown in Fig. 3c–f and Fig. S13 (ESI†), TCF3333 has the highest PLD_{max} (The max value of PLD) of the four TCF films, followed by TCF4444 with the second-highest PLD_{max}, which is consistent with the theoretical calculations of the RL. TCF1111 and TCF2222 have the lowest PLD_{max}, indicating the poorest ability to attenuate EM waves. All possible combinations were simulated and shown in Fig. S14 (ESI†), and all colormaps are drawn using the same scale. Summarizing the simulations of the films with four-layer structures, the top two PLD_{max} values obtained were for TCF1423 and TCF2413, as depicted in Fig. 3g–h. TCF4123 and TCF4213 are shown together in Fig. 3i–j. The specific PLD_{max} values are shown in Fig. S15 (ESI†). Multiple combinations are found to achieve a PLD_{max} far exceeding that of TCF3333, with the optimal combination TCF1423 showing a 58.7% increase compared to TCF3333. For all 24 permutations, one common point is that the position of the

Fig. 2 TCF film bonding process.

strongest PLD value is always at the layer where TCF3 is located, indicating that TCF3 primarily serves as the loss layer in the four-layer structure. A single TCF layer in the four-layer films shows a significant enhancement in the PLD value compared to a single TCF layer in homogeneous TCF films. This means that the construction of the structure promotes the enhancement of the loss capacity of the original TCF layer. As shown in Fig. S16–S23 (ESI†), all of the EM field simulations can be generally divided into four categories. When the first layer is set as TCF1 or TCF2, the transmission state of the EM field is similar due to the low reflection of the EM wave. TCF3 and TCF4 have stronger attenuation capabilities, and can interact strongly with EM waves. Based on the best four TCF structure thin films, a waveguide method was used to measure the EM parameters and the S parameters of the four-layer films. Because of the existence of the multilayer structure, the S parameter of the film is different from that of the homogeneous film, which leads to many negative electromagnetic parameters obtained by back extrapolation (Fig. S24, ESI†). The obtained S parameters of the heterogenous films are shown in Fig. 3k–n, and each of them exhibits a huge difference between $S11$ and $S22$, where $S11 < S22$ in most frequency ranges. The similarity between $S21$ and $S12$, which are used as transmission coefficients, indicates that the transmittivity of the EM wave is less affected by the multilayer structure. The smaller $S11$ values are associated with the construction of the structures, and being lower than the $S22$ values means higher absorption of EM waves. When comparing the RL related to $S11$ and $S22$ (Fig. S25, ESI†), the RL value of TCF1423 at 11.81 GHz is reduced by 6.45 dB, and that of TCF2413 at 11.74 GHz is reduced by 6.07 dB, thus realizing an enhancement of low EM wave absorption. TCF1423 and TCF2413 achieve bandwidth expansions of 8.72–9.56 GHz and 10.26–12.09 GHz, respectively. For the films with optimal performances, the RL and IM were calculated and are shown in Fig. S26a–h (ESI†). Compared to a homogeneous TCF film, the IM of the four-layer films was greatly optimized. All of the films exhibit IM values in the range of 0–2, realizing the effective introduction of EM wave, guaranteeing the improvement of EM wave absorption performance. For TCF4123 and TCF4213, the best IM value is not found in the same position, which leads to a difference in the absorption peak location. According to the PLD, a pure impedance gradient may not be optimal. Taking TCF1243, TCF2143, TCF2431 and TCF4312 as examples, they are all based on pure impedance gradients, but the performance of TCF4 in these combinations is much lower than those of other combinations. Optimal performance is limited by the loss capability of TCF3. Based on the above work, a new idea for the design of an impedance gradient can be obtained, that is, the top layer still devotes itself to the introduction of the EM wave, the back layer should still reflect much of the incident EM wave, however, the interlayer does not require a continuous gradient in loss capability.

In summary, an effective way to prepare EM wave absorption films to achieve high EM wave absorption performance and high recovery performance is to use TPE as the substrate. The construction of multilayer films needs to include the following key elements: a strong absorption element, an impedance matching element and a transition element. In this general design, the performance of the multi-layer structure could be determined by the layer with the greatest loss to EM waves and that layer is often placed as the last layer. The first layer usually consist of a material with excellent IM, enabling low reflection and impedance optimization of EM waves. The tuneable intermediate layers have a great influence on the absorption peak and EM wave absorption characteristics (Fig. S27, ESI†). When there is a high-low-high impedance transition inside the film, the electromagnetic wave tends to be limited to multiple reflections inside the film, thus achieving higher attenuation performance. In this work, a combination of simulation an experimental work is used to improve the performance of four-layer films. The general mechanism can be summarized in two points: (a) by enhancing the introduction of the EM waves, the loss capability of a single layer can be enhanced and (b) by combining multiple layers of a material, multi-layer loss is enhanced simultaneously. This work demonstrates the preparation of multilayer films by enhancing the interlayer bonding *via* physical interactions, which lays a foundation for the construction of more complex multilayer films with high-efficiency EM wave absorption performances and recyclable properties.

Data availability

The data supporting this article have been included as part of the ESI.†

Conflicts of interest

There are no conflicts to declare.

Notes and references

1 Z. Huang, J. Cheng, H. Zhang, Y. Xiong, Z. Zhou, Q. Zheng, G. Zheng, D. Zhang and M. Cao, *J. Mater. Sci. Technol.*, 2022, **107**, 155–164.
2 L. Liang, W. Gu, Y. Wu, B. Zhang, G. Wang, Y. Yang and G. Ji, *Adv. Mater.*, 2022, **34**, 2106195.
3 Y. Z. Wang, Y. C. Wang, T. T. Liu, Q. L. Zhao, C. S. Li and M. S. Cao, *Nano-Micro Lett.*, 2025, **17**, 65.
4 W. Q. Cao, Z. Z. Wang, X. Wan, T. T. Liu, C. B. Cao and M. S. Cao, *Adv. Compos. Hybrid Mater.*, 2024, **7**, 187.
5 Y. Deng, B. Ren, Y. Jia, Q. Wang and H. Li, *J. Mater. Sci. Technol.*, 2024, **196**, 50–59.
6 H. Yao, J. Yang, H. Li, J. Xu and K. Bi, *Adv. Compos. Hybrid Mater.*, 2023, **6**, 43.
7 W. Jiang, H. Qian, Q. Cao and B. Jiang, *Compos. Commun.*, 2024, **46**, 101829.
8 C. Mai, N. Huang, M. Gao, Y. Sun, J. Yan, C. Zhai and W. Zhao, *J. Alloys Compd.*, 2023, **968**, 171960.
9 B. Quan, Y. Chen, Y. Wang, X. Lu, T. Guo, M. Zhang and X. Huang, *Carbon*, 2023, **206**, 392–401.
10 Y. Heng, X. Qi, L. Xu, Y. Yan and Q. Ni, *Polym. Compos.*, 2024, **45**, 8710–8720.
11 B. Quan, W. H. Gu, J. Q. Sheng, X. Lv, Y. Mao, L. Liu, X. Huang, Z. Tian and G. Ji, *Nano Res.*, 2021, **14**, 1495–1501.
12 Q. Zheng, J. Q. Wang, W. Q. Cao, H. Z. Zhai and M. S. Cao, *Adv. Funct. Mater.*, 2024, 2417972.
13 Q. Huang, G. Wang, M. Zhou, J. Zheng, S. Tang and G. Ji, *J. Mater. Sci. Technol.*, 2022, **108**, 90–101.
14 H. Zheng, H.-P. Shao, T. Lin, Z.-F. Zhao and Z.-M. Guo, *Rare Met.*, 2018, **37**, 803–807.
15 N. Lu, J. Xu, M. Yuan and G. Sun, *Nano Res.*, 2024, **17**, 3324–3333.
16 L. Kong, S. Luo, G. Zhang, H. Xu, T. Wang, J. Huang and X. Fan, *Carbon*, 2022, **193**, 216–229.